Helicopter Noise Reduction by Individual Blade Control (IBC) - Selected Flight Test and Simulation Results -

W. R. Splettstoesser, K.-J. Schultz, B. van der Wall, H. Buchholz
Deutsches Zentrum für Luft- und Raumfahrt (DLR), Lilienthalplatz 7, 38108 Braunschweig, Germany

W. Gembler, G. Niesl
Eurocopter Deutschland GmbH (ECD), 81663 München, Germany

A collaborative flight test programme was conducted to study among other objectives the potential of open-loop Individual Blade Pitch Control (IBC) to reduce the external noise of a helicopter in partial power descent, a flight regime known to generate the highly annoying Blade-Vortex Interaction (BVI) impulsive noise. The blade root control system employing actuators in the rotating frame, was installed on a BO 105 helicopter, which was flown over an extended linear microphone array. The acoustic measurements on the ground were synchronised to the flight track and rotor performance measurements supplemented by limited simultaneously acquired on-board acoustic and blade surface pressure data. Selected test results quantifying the noise reduction potential of the IBC technique, are presented and compared to numerical rotor simulation results calculated by the aeromechanic S4 code and the acoustic AKUROT code of the DLR. A significant noise reduction benefit (exceeding 5 dB) of the maximum A-weighted (BVI) noise level was obtained for the 2/rev IBC mode; further, over a wide range of IBC phase angles simultaneous noise and vibration reductions were observed. The complete data base acquired will contribute to the development and validation of a fast control algorithm for closed-loop IBC applications.

Introduction

Annoyance level and public acceptance of present days helicopters approaching heliports or landing pads in populated areas are strongly affected by blade-vortex interaction (BVI) impulsive noise dominating the external noise radiation during partial power descent and landing. BVI occurs when a rotor blade closely passes or directly encounters the blade-tip vortices shed by preceding blades, giving rise to impulsive noise radiation directed downwards from the rotor plane as well as to vibrations transmitted to the fuselage. The intensities strongly depend on flight velocity and rate of descent. Over the years, several attempts to reduce BVI noise and vibrations by modification of the blade-tip area have been performed with limited success [1]. But the research over the past decades has substantially improved the physical understanding of the BVI noise mechanisms and also of controlling techniques, particularly of active rotor control technology [2].

It has well been recognised that active blade root pitch control of a helicopter rotor represents an effective technique – either in form of higher harmonic control (HHC) or as individual blade control (IBC) – to reduce the impulsive BVI noise during partial power descent and landing approach.

Paper No.30, presented at the RTA – AVT Symposium, Braunschweig, Germany, 8 – 12 May 2000

HHC is based on a blade pitch control law depending on restricted multiples of the rotor rotational frequency (i.e. n/rev and (n ± 1)/rev of an n-bladed rotor) while IBC additionally allows for arbitrary pitch control inputs. Extensive model rotor wind tunnel tests employing higher harmonic blade pitch control (HHC actuators placed in the fixed frame acting on the fixed part of the swashplate) and some flight tests on a Gazelle SA 349 helicopter have demonstrated a significant noise reduction potential of about 6 dB for open-loop HHC, however, at elevated vibratory forces [3, 4, 5, 6]. It was found that, for optimum noise control at different operational flight conditions, different HHC schedules were necessary, thus requiring closed-loop HHC with optimised control algorithms. By application of this technique, noise reductions could be achieved without increase of vibrations [7].

A promising alternative to HHC offers IBC where the pitch actuators are placed in the rotating frame, thus allowing both unrestricted multi-harmonic blade pitch variations and arbitrary pitch motion for each individual blade. Initial flight tests on a BO 105 helicopter [8, 9] and comprehensive wind tunnel full-scale tests employing the BO 105 main rotor in the 40 by 80 foot wind tunnel of NASA Ames [10, 11], have shown a noise benefit exceeding 6 dB (in the wind tunnel test) at simultaneously reduced vibratory loads. For safety

Paper presented at the RTO AVT Symposium on "Active Control Technology for Enhanced Performance Operational Capabilities of Military Aircraft, Land Vehicles and Sea Vehicles", held in Braunschweig, Germany, 8-11 May 2000, and published in RTO MP-051.

reasons, in these early (1990/91) flight tests, the IBC input was restricted to 0.42° amplitude so that the full capability of the IBC system could not be completely explored; however, for the wind tunnel tests, an improved blade root control system was employed.

To fully explore the potential of the IBC technology concerning the reduction of external (BVI) noise, cabin vibration, and power required, the ongoing Rotor Active Control Technology (RACT) programme was launched being jointly conducted by Eurocopter Deutschland (ECD), the German Aerospace Center (DLR), the Daimler Benz Research Establishment (DB), the Technical University of Braunschweig, and ZF-Luftfahrt (ZFL). Alternatively to the blade root control concept, in a parallel activity, a smart actuation concept with trailing edge flaps is developed and investigated in a wind tunnel; more details of the RACT programme are given in [12, 13].

One major RACT milestone was the conduct of open-loop IBC flight tests with extended noise measurements on ground employing the upgraded BO 105 IBC demonstrator with the major objectives to generate a comprehensive data base for (1) the development of control laws for closed-loop IBC applications, (2) the verification of existing full-scale rotor wind tunnel results, and (3) the quantification of the noise reduction potential of IBC on a real helicopter and the validation of rotor aeroacoustic numerical simulations including IBC effects.

This paper is focussed on the third objective and addresses the experimental approach, rotor aeroacoustic simulations, and comparisons of flight test and simulation results. Further accomplishments of this open-loop IBC flight test concerning other objectives are provided in separate papers [14, 15, 16].

Experimental Approach

IBC Flight Tests

Open-loop IBC flight tests were conducted in March/April, 1998 to explore the potential of the IBC technology under real flight conditions. An upgraded IBC system (± 1.2° pitch control authority) developed by ZFL and extensive measurement and data acquisition equipment provided by ECD, DLR, and DB were installed on the experimental BO 105 S1 helicopter shown in flight in Figure 1. The key component of the IBC system is a servo-hydraulic actuator that replaced the conventional rotating pitch links of the main rotor. Additional components of the IBC system include hydraulic and electric sliprings, hydraulic components, and a digital controller. Safety of flight is guaranteed by an emergency shutdown feature that locks the actuators mechanically if hydraulic pressure drops. The IBC hydraulic system is separated from the helicopter hydraulics and can be shut down manually or automatically. A detailed description of the IBC system is given in [9].

Figure 1 IBC demonstrator BO 105 S1

Highly complex data acquisition systems on board of the IBC demonstrator rotorcraft and on the ground were employed for simultaneous measurements of operational parameters, vibrational forces, blade surface pressures, the helicopter positions, and the emitted noise on board and on the ground.

Objectives and Test Plan

The main objective of the open-loop IBC flight tests was the acquisition of a comprehensive acoustic, aeromechanic, and flight operational data base which were to be analysed under different aspects and is used:

(1) to develop a fast and stable control algorithm for a closed-loop IBC system capable of simultaneous noise and vibration reduction over the total flight envelope.

(2) to test and evaluate a closed-loop controller concept for vibration reduction. The analysis of the flight test data regarding this goal is communicated in [14].

(3) to study different BVI identification algorithms under real flight conditions. Results concerning this goal are presented in [15].

(4) to verify existing IBC wind tunnel results by careful analysis of the flight test results. The accomplishments regarding this objective are discussed in [16].

(5) to quantify the noise reduction potential of IBC on a real helicopter and to validate an aeroacoustic numerical simulation approach taking into account IBC effects. The analysis and comparison of the flight test and simulation results concerning this goal are provided and discussed in the present paper.

The test plan was designed to identify and cover flight conditions with intensive BVI noise generation. For a systematic variation of IBC parameters, a 6°-descent flight at nominal 65 kts IAS (ICAO approach) was chosen. Since there was little experience available for arbitrary IBC inputs (e.g. wavelets), harmonic IBC inputs of 2/rev, 3/rev, 4/rev, and 5/rev and some mixed-mode inputs were tested. A nominal IBC amplitude of ± 1° was used except for 3/rev for which a control amplitude of 0.5° was selected. Furthermore, for the 2/rev IBC mode, a variation of the control amplitude between 0.4° and 1.0° was examined.

On-board Test Equipment

Additionally to the IBC system, a sophisticated experimental system has been integrated in the helicopter, which is described in detail in [13] and summarised here.

The instrumentation in the rotating system comprises 19 pressure transducers embedded in one blade, 3 accelerometers each on the hub and at the blade tip, 2 strain gauges on each blade for flapping and lead lag moment and further sensors used in the actuation system. The data are conditionally sampled at a rate of 512/rev triggered by a rotor azimuth angle encoder. A fast interface computer collects and transmits the data via slipring to a control computer (called IBIS) located in the fixed system. IBIS also collects all data from the basic instrumentation and transmits via telemetry safety critical signals as well as data reflecting the control activity and the flight states to the ground station. For eventual use in the noise controller, three microphones are mounted on the starboard landing skids. To ensure accurate flight trajectory measurements, a GPS–receiver as part of a DGPS system is installed on-board, which communicates by its own telemetry with the GPS reference station on ground.

Acoustic Measurements on Ground

Flyover noise measurements were conducted by use of an extended linear microphone array arranged perpendicular to the flight track centreline covering a range of ± 300 m as shown in Figure 2.

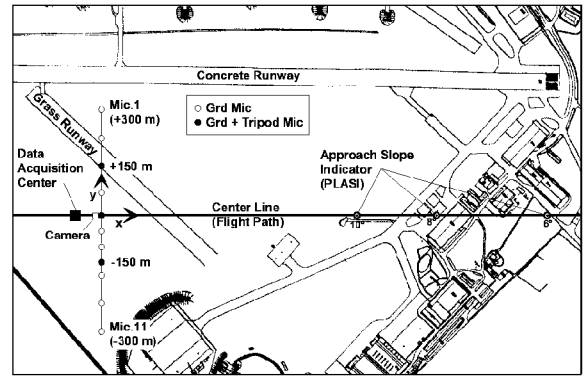

Figure 2 Test set-up on Dornier-Fairchild airfield showing microphone array and coordinate system

The microphone array consisted of 11 ground microphones and 3 microphones mounted on tripods 1.2 m above the ground at the ICAO noise certification positions 0 m and ± 150 m. The ground microphones were placed in an inverted position 7 mm above a circular metal plate (of 0.4 m diameter) out of the centre at 0.75 radius, to minimise reflection influences. For better resolution of the important advancing side BVI noise radiation, a smaller spacing of ground microphones was chosen on the starboard side of the helicopter in approach.

A photo camera was set up 15 m apart from the central microphone and used to determine the overflight height and the exact overflight time in terms of GPS time. Exact flight path co-ordinates, speed over ground, and flight path angles were acquired by a differential GPS system with the reference GPS receiver located at the acoustic data acquisition centre on ground (50 m away from the central microphone). Unfortunately, in a number of test runs, the DGPS system did not properly work. In these cases, the on-board recorded pressure altitude history and the photometric overflight height was used to evaluate the validity

of the test run concerning the flight path. All 14 signals of the ground based microphones were simultaneously acquired by the central acoustic data acquisition system (Figure 3).

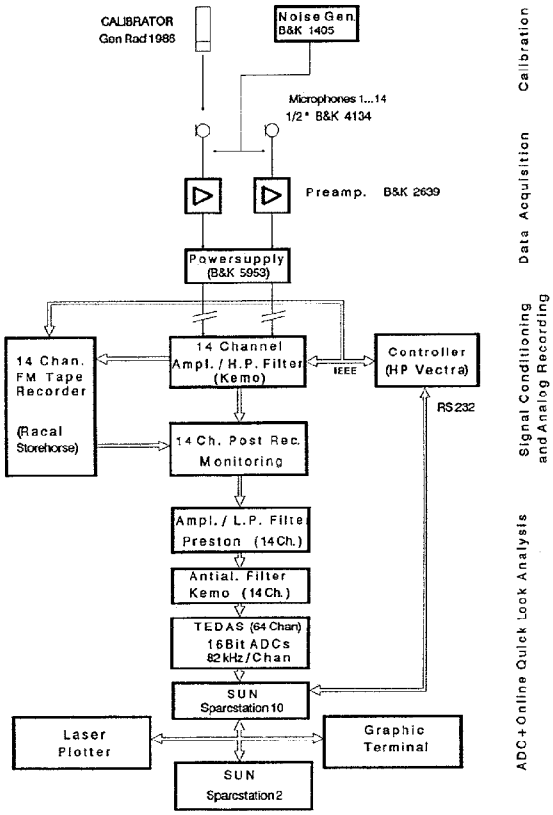

Figure 3 Acoustic data acquisition scheme

After PC-controlled signal conditioning, the data were recorded analogously on an FM tape recorder and, in parallel, were digitised at a rate of 14 336 Hz and 16 Bit resolution giving a useful frequency range of about 7 000 Hz, which is sufficient for meaningful full-scale helicopter noise analysis. A powerful workstation allowed to record and store the digitised data of all channels for complete overflights up to 90 seconds. In addition, the GPS data and the atmospheric data from the on-site weather station (2 m above ground) were recorded. On-line calculations provided "quick-look" graphic output of weighted sound pressure level histories and noise contours as well as flight trajectories that allowed evaluation of the validity of the test data.

Synchronisation of the acoustic, flight path and on-board data was established via the common GPS time and the recording of that instant in time when the camera took a picture of the helicopter in its overflight position.

Test Conduct

The open-loop IBC flight tests were conducted in March/April, 1998 on the Dornier-Fairchild airfield in Oberpfaffenhofen near Munich. Each test series was started with the helicopter mass corresponding to the maximum take-off mass of 2 300 kg. Refuelling was mandatory after 10 per cent loss of mass. A very useful tool to guide the test pilot during the different approach flights was a powerful Pulse Light Approach Slope Indicator (PLASI) provided by Dornier Fairchild. The reference overflight height of 120 m was kept constant for all approach flights. For these landing approach flights, synchronous recording of the acoustic and flight path data started at least 1 200 m before the microphone array and ended about 500 m behind it to ensure recording of the noise maximum and the "10 dB-down" points particularly at the outer microphones. Synchronised on-board data were acquired over a period of 5 seconds when the helicopter was approaching and passing the microphone array.

Data Evaluation and Correction

After careful evaluation of the acoustic, the flight path and rotor operational data, in particular, of flight path angle, rotor tip path angle, collective and cyclic pitch in the important acoustic "10 dB-down" period, a number of test runs had to be excluded from further analysis. Since the flight test period was restricted, the number of valid flights per test condition is rather limited and the variance of the noise levels is rather high, probably a consequence of partly unfavourable wind conditions and different test pilots involved in the flight tests. Therefore, the noise levels are presented in terms of mean values with indication of the 90 per cent confidence intervals for each test condition.

The measured acoustic data shown in this paper have been corrected to reference flight path or, if not available, to the reference overflight height and to the International Standard Atmosphere (ISA + 10°C) sea level conditions.

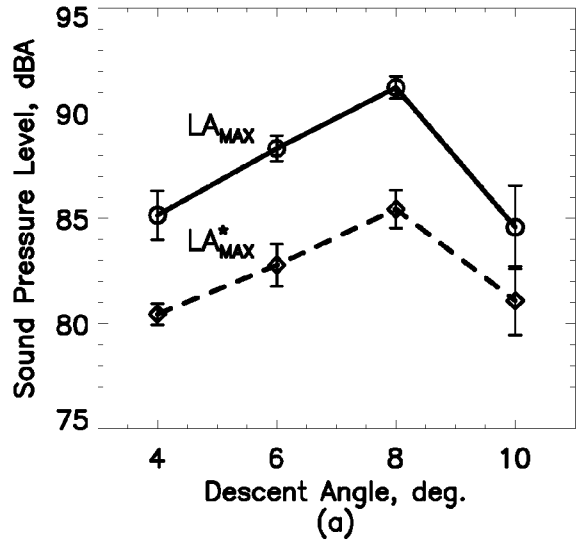

Acoustic Results and Analysis

Variation of Descent Angle

A small part of the flight test was devoted to baseline (no IBC) descent flight conditions to determine the flight path angle range where BVI impulsive noise radiation is most intense for the BO 105 main rotor. The result, in terms of A-weighted noise levels (LA), of the descent angle sweep at constant speed of 65 kts IAS is shown in Figure 4.

In Fig. 4 (a), the maximum noise level LA_{MAX} of the ground microphones and the maximum noise level of the 11-ground microphone average (energetic average) LA^*_{MAX} are plotted versus descent angle, while in Figs. 4 ((b)-(e)), the A-weighted noise contours with the helicopter in the central position are presented marked by a

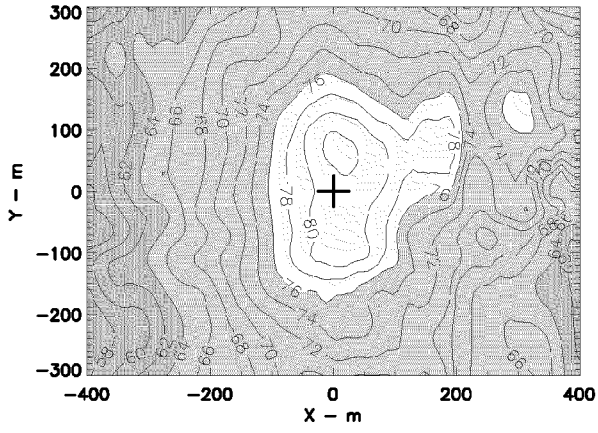

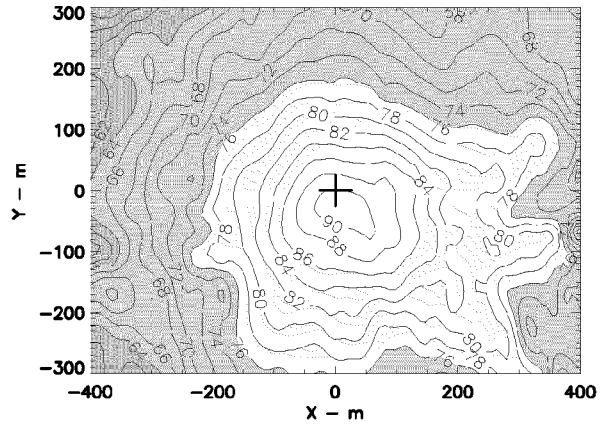

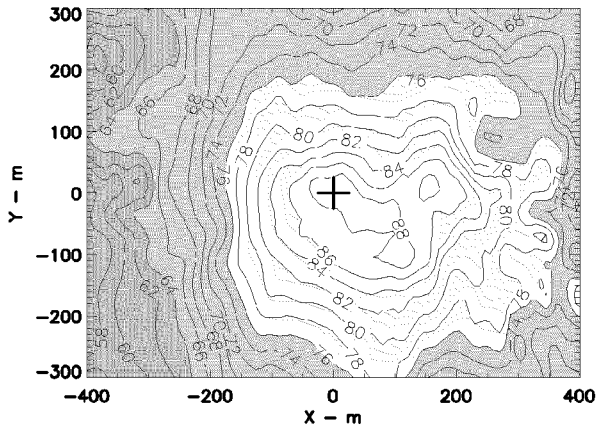

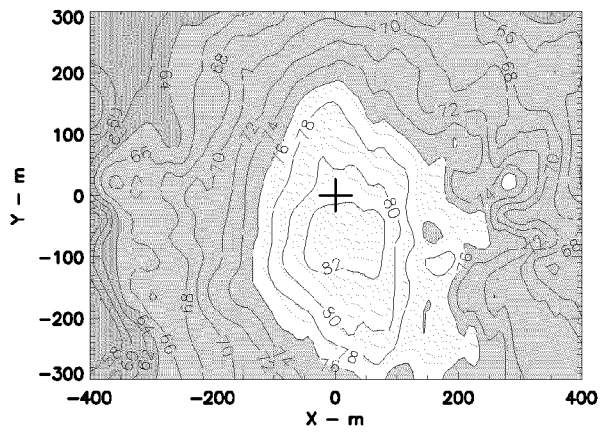

Figure 4 A-weighted noise levels (a) and noise contours (b-e) for different descent angles at nominal 65 kts IAS without IBC activated

cross. Noise intensities and directivities correspond well with scaled model rotor wind tunnel results [17], where the maximum BVI noise radiation was identified for a descent angle between 6 and 7°. Maximum intensities are focussed below the helicopter on a pattern extended slightly forward and towards the advancing side of the main rotor. Increased descent angles mean increased backward tilt of the rotor tip-path plane and a change of the BVI encounters towards smaller azimuth angles; consequently, the radiation patterns for 8° and 10° show maximum intensities more downstream (at smaller X) and more extended on the advancing side (larger neg. Y) compared to the 6-degree case.

IBC Variations

For investigation of the IBC effects on noise and vibrations, the 6-degree descent ICAO approach at fixed 65 kts flight velocity was selected. As stated earlier, only higher harmonic pitch control laws have been tested.

2/rev Phase Variation: The results for 2/rev IBC phase variation at increments of 30° and 1° amplitude are presented in Figures 5 through 8. The noise reduction benefit in terms of ΔLA_{MAX} as well as of ΔLA^*_{MAX} and SEL* is shown in Fig. 5 (a) and Fig. 5 (b), respectively.

Like in the full-scale rotor wind tunnel test [10, 11], a significant BVI noise reduction is seen over a large range of phase angles. Minimum noise radiation (optimum reduction up to nearly 6 dBA for LA_{MAX}) is achieved in the phase angle range $170° \leq \phi_2 \leq 250°$, while a secondary minimum is found in the range between $45° \leq \phi_2 \leq 75°$. Increased levels have been measured for the phase angles ranging from $290° \leq \phi_2 \leq 30°$. The vertical bars indicate the 90 per cent confidence interval (u_{90}) within which, with 90 per cent probability, the "true" value for a specific test condition can be expected. Similar results are obtained for the Sound Exposure Level, SEL*, and LA^*_{MAX}, the noise measures based on 11-microphone averages (Fig. 5 (b)). Corresponding A-weighted noise contours for the baseline (no IBC) case and for two specific IBC phases $\phi_2 = 201°$ (minimum BVI noise) and $\phi_2 = 52°$ (secondary minimum) are compared in Figures 6 ((a)-(c)). A distinct reduction of high-intensity BVI noise radiated to the heliport neighbourhood can be achieved for both in flight direction and in lateral direction. In Figure 7 ((a) and (b)), the sound pressure histories for one rotor revolution, measured by the central

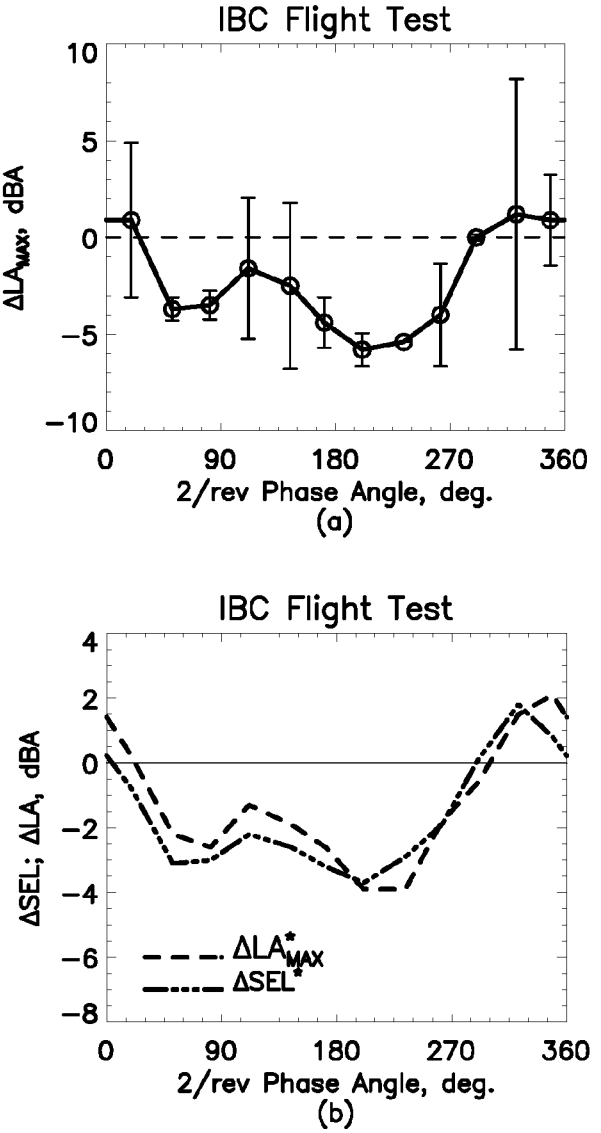

Figure 5 Effect of 2/rev IBC phase variation ($\theta_2 = 1°$) on A-weighted noise levels for 6°-descent flight at 65 kts IAS referenced to the baseline case without IBC, (a) $\Delta LA_{MAX} \pm u_{90}$, (b) ΔLA^*_{MAX} and Δ SEL*

ground microphone, are illustrated for the baseline case (part (a)) and for minimum noise control (part (b)). A significant reduction of the impulsive content of the typical BVI noise signature is obvious, which is directly correlated with a smoothed blade surface pressure time history on the advancing side, as illustrated in Figure 8 for a leading edge (3 per cent chord) pressure sensor at r/R = 0.7. The comparison of the baseline case with the minimum noise case indicates that the blade-parallel BVI's on the advancing side in the azimuth range between 30° and 60° have been largely suppressed by IBC, which is the case on the retreating side between 300° and 330° as well.

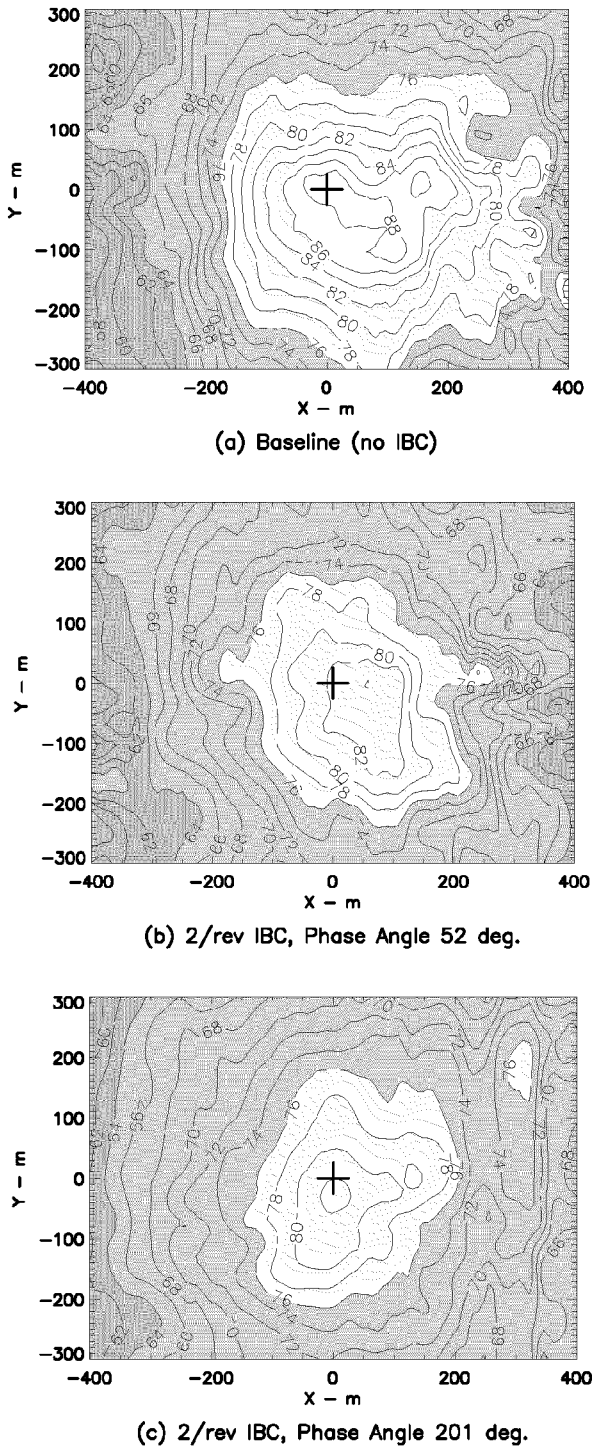

Figure 6 A-weighted noise contours for (a) baseline case (no IBC) and for selected 2/rev IBC-phase settings (θ_2 = 1°) of (b) ϕ_2 = 52° (secondary minimum noise) and (c) ϕ_2 = 201° (minimum noise). Flight condition as for Fig. 5

2/rev Amplitude Variation: Increasing the 2/rev amplitude from 0.4 to 1.0° in increments of 0.2° at a fixed phase angle of 60° resulted, as expected, in

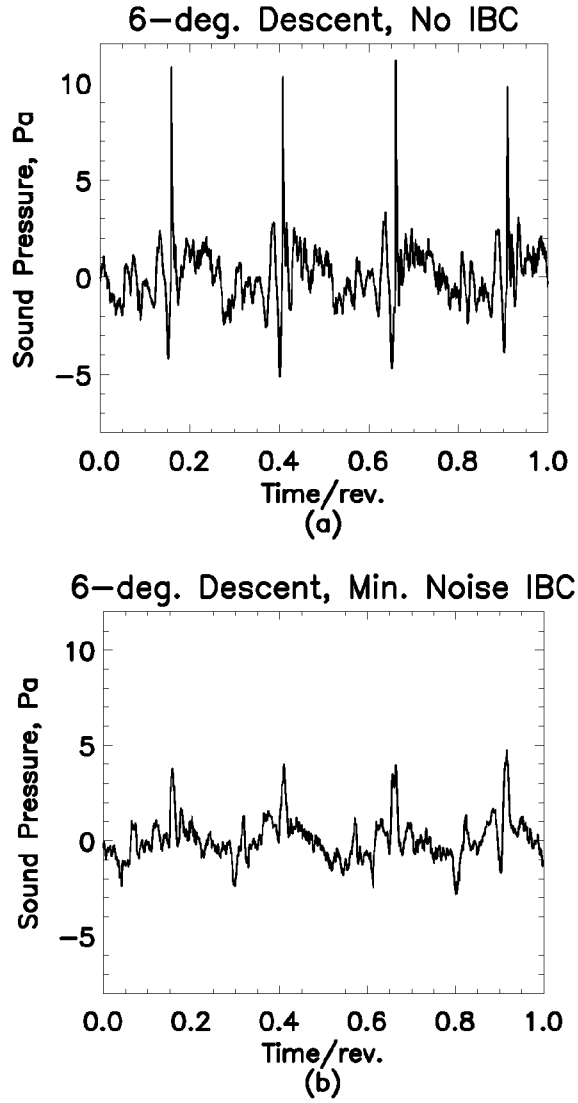

Figure 7 Sound pressure histories at maximum immission points for (a) baseline case (no IBC) and for (b) minimum noise IBC settings (2/rev, θ_2 = 1°, ϕ_2 = 201°. Flight conditions as for Fig. 5

increasing acoustic benefit as shown and discussed in [16], however, in a non-linear way. Corresponding leading edge blade pressure histories showed indeed an increase in retreating side BVI for amplitudes 0.6° and 0.8°, which was not measured for 0.4° and 1.0°. This may have been caused by extraordinary rotor trim changes required due to unfavourable wind conditions prevailing during these test runs with retreating side cross and tail wind speeds partly exceeding the ICAO limits. Furthermore, due to the small number of test runs per condition, the confidence level is rather poor from a statistical point of view.

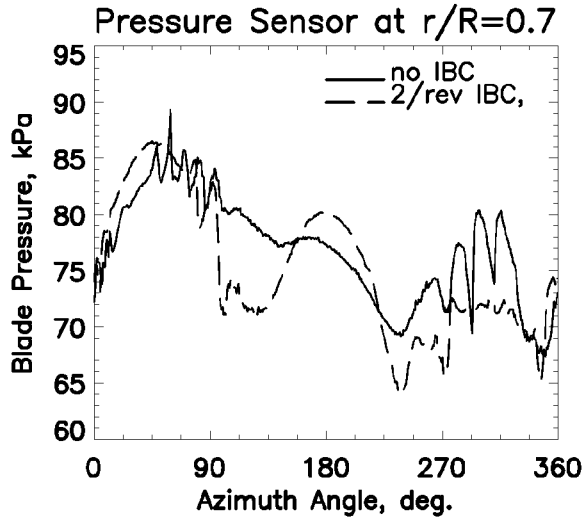

Figure 8 Leading edge (0.03 c) absolute blade surface pressure histories for the baseline case (no IBC) and for minimum noise IBC setting (2/rev, $\theta_2 = 1°$, $\phi_2 = 201°$). Flight conditions as for Fig. 5

3/rev and Mixed-Mode IBC Variations: Results of 3/rev and mixed mode IBC phase variations are shown in section "Comparison of Simulation and Flight Test Results".

Rotor Aeroacoustic Simulation

The DLR rotor code S4 here is used to compute the effects of active control (HHC, IBC) on the rotor dynamic forces and its acoustic emission via high-resolution blade air loads [18, 19]. It mainly consists of three modules: the aerodynamics, the structural dynamics and the induced velocities module, embedded in a trim algorithm [20]. The rotor is trimmed to prescribed values of thrust and hub moments from experiment by variation of the collective and cyclic controls. The acoustic postprocessing is done by using the high-resolution load distribution of the S4 program as an input for the Ffowcs-Williams and Hawkings equation. The program scheme is sketched in Figure 9.

For simulation of the IBC cases, the following combination is used: non-linear unsteady aerodynamics including yaw; hingeless blades with 3 flap modes, 2 lead-lag modes and 1 mode in torsion; prescribed wake geometry including HHC effects. For analysis of the IBC effects on the BO 105 main rotor noise emission, a typical rotor condition at 6°-descent flight is chosen from the experiments. This provides data for thrust, rotor roll and pitch moments, advance ratio, and shaft angle of attack. Then, the S4 code is run for this

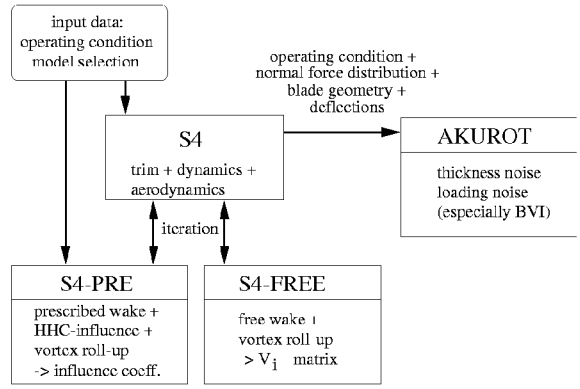

Figure 9 Computational scheme for rotor simulation and acoustic emission

baseline case (no IBC) first. The wake geometry and blade dynamics simulation is iteratively performed; typically 2 iterations are enough to obtain convergence. In this test campaign, the IBC input schedules followed the higher-harmonic blade pitch control law: $\theta = \theta_n \cdot \cos(n\psi - \phi_n)$, where θ_n denotes the amplitude, n the multiple of the rotational frequency, ψ the azimuth angle, and ϕ the phase angle. IBC variations are calculated in the similar way as the baseline case, namely prescribing the control angle ($\theta_2 = 1°$) and its phase ($\phi_2 = 0°, 30°, \ldots 330°$) and trimming again to thrust and moments of the baseline condition as the pilot did when flying the helicopter.

Comparison of Simulation and Flight Test Results

Baseline Case (no IBC) Comparisons

Since the aerodynamics of the S4 code essentially are based on lifting line theory, no pressure distribution is available from the code. On the other hand, due to scarce instrumentation of the BO 105 rotor blade, no local loading nor blade deflections are available for direct comparison. However, the blade's leading edge pressure distribution can be obtained from the transducers at 0.03c (c = blade chord length) of the upper surface between 0.6R and 0.97R. They are very sensitive to changes of oncoming flow conditions and thus are useful indicators for BVI events, provide information wether the vortices are flying above or below the rotor disk, and where they are closest to the blades. When applying a high-pass filter suppressing the lowest fluctuations (< 6/rev) that contain mainly dynamic pressure and blade motion components, the remaining pressure distribution is

originating mainly from BVI events, i.e. the upwash and downwash of individual vortices coming close to the blade's leading edge. This can be compared to the computed induced velocity distribution, filtered in the same way.

In Figure 10, the baseline case pressure distribution of one individual revolution from the flight test indicating the BVI geometry (Fig. 10 (a)) is compared to the BVI locations resulting from the simulation (Fig. 10 (b)).

The simulation predicts the vortices close to the rotor blades at the most critical locations for BVI noise emission, i.e. where the vortices are parallel to the rotor blade's leading edge (see [15]). The flight test, however, does not show this in that detail; here the vortices do pass the disk earlier, i.e. at azimuths of about 70° on the advancing and at 280° on the retreating side. Changing the flight path angle to 4°- descent, the simulation (Fig. 10 (c)) gives BVI locations that compare much better to the flight test, especially on the advancing side. Similar observations were made when wind tunnel and flight test results were compared [21]. One probable reason for this behaviour may be found in the wind conditions during the test, resulting in an instantaneous effective flight path that was slightly different from the geometrical flight path. Another reason for the differences in the BVI locations may be seen in the assumption of the basic wake geometry with rotor moments near zero, a trim condition that has been used in the HART [6] test in the DNW wind tunnel and for the code validation. In the flight test, a strong pitch moment in the range of 2000 Nm was measured, and the lift for that moment must have been created about 80° earlier in azimuth. Following the assumptions of momentum theory, this will cause extra downwash on the advancing side and some upwash on the retreating side relative to a condition with zero moments. Tip vortices thus will be convected more downwards on the advancing side and the BVI locations will shift to larger azimuth positions. Whatsoever, as a reference for the simulations, the 6°-descent condition was chosen and the changes of the wake structure relative to this baseline case resulting from IBC variations are the important features to represent.

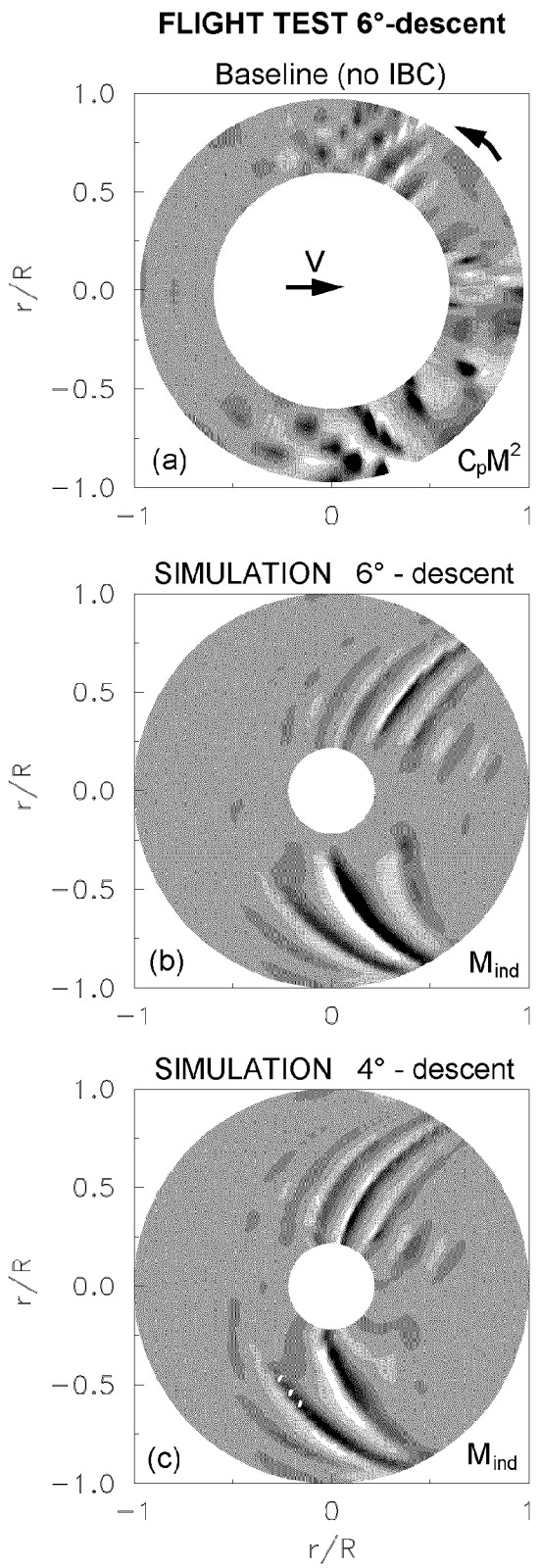

Figure 10 Comparison of (a) the measured leading edge blade pressure distribution C_pM^2 of the flight test at 6°-descent to computed induced velocity distributions M_{ind} for (b) 6°-descent and (c) 4°-descent flight at nominal 65 kts IAS; data h.p. filtered at 6/rev

Comparison of IBC effects

For analysis of 2/rev IBC effects on the rotor noise emission, the flight condition and steady rotor forces and moments from the baseline case are kept constant but, additionally, an IBC control

angle of $\theta_2 = 1°$ is applied with a phase varying from $\phi_2 = 0°$ to 360°. This does basically change the low-frequency content of the loading distribution but also affects the vortex flight paths through the rotor disc and, thus, the BVI locations via the prescribed wake. Therefore, the high-frequency content of the blade loading also is affected, and may result in different noise emission characteristics.

2/rev IBC comparisons: The A-weighted maximum noise levels measured on ground and those computed from the simulated loading distributions are compared to each other in Figure 11 (a). The computed noise levels appear to have a phase shift of about 20° relative to the experiment but the essential behaviour of noise emission or reduction with 2/rev IBC phase variation is well predicted.

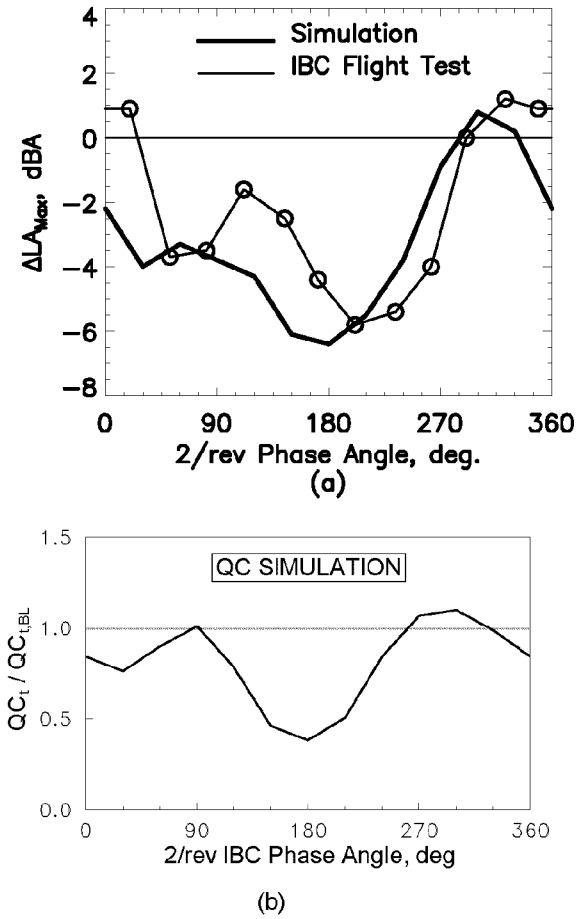

Figure 11 Comparison of (a) measured and computed A-weighted maximum noise levels with (b) calculated acoustic quality criterion for 2/rev IBC phase angle variation ($\theta_2 = 1°$). Flight conditions as for Fig. 5

In the time domain, a BVI noise quality criterion based on the blade's leading edge pressure was developed as an indicator for the noise emission measured on ground [15]. This principle can also be applied to the unsteady simulated rotor blade loading, based on the non-dimensional normal force distribution $C_nM^2(r, \psi)$. Therein the azimuthal gradient of the loading is multiplied by weighting functions W_β and W_M, representing approximately the effect of the blade-vortex interaction angle and the local Mach number on noise intensity. The result of this quality criterion is given in Fig. 11 (b).

It is obvious that for most of the IBC control settings, a significant reduction of the predicted BVI noise level as well as of the acoustic quality criterion is achieved, with a minimum at $\phi_2 = 180°$ and a secondary minimum at 30°, while a slight increase is indicated at 90° and between 270° and 330° phase angle. Compared to the noise levels measured on ground, this curve appears to have the same shift of about 20° as the predicted noise curve (Fig. 11 (a)) but the essential features are represented. In terms of rotor azimuth, this shift reduces to half the value, and is within the uncertainty of the HHC wake deflection algorithm used for the prescribed wake approach. In Figure 12 ((a) and (b)), measured and predicted A-weighted noise contours are compared for the baseline (no IBC) 6°-descent case and for the minimum noise 2/rev IBC setting of Fig. 11.

Flight test and simulation results regarding noise directivity and level are in quite good agreement. It should be noted here that the simulation results have been corrected for the ground effect by adding 6 dB to the calculated values. The levels are underpredicted in lateral direction, probably an effect of the missing tail rotor noise contribution.

The behaviour of hub vibrations does exhibit a similar phase shift as was found for the noise predictions [15]. An important and promising result of the 2/rev IBC variations was identified in the phase range between $330° < \phi_2 < 70°$, where both noise and vibrations simultaneously are reduced. This is in favourable contrast to 3/rev HHC variations examined in the HART test [6], where vibrations were large when the noise was low and vice versa.

At the minimum of the calculated LA_{MAX} function corresponding to the minimum of the quality criterion ($\phi_2 = 180°$), the measured pressure distribution is compared again to the induced velocity distribution from simulation. This is shown in Figure 13.

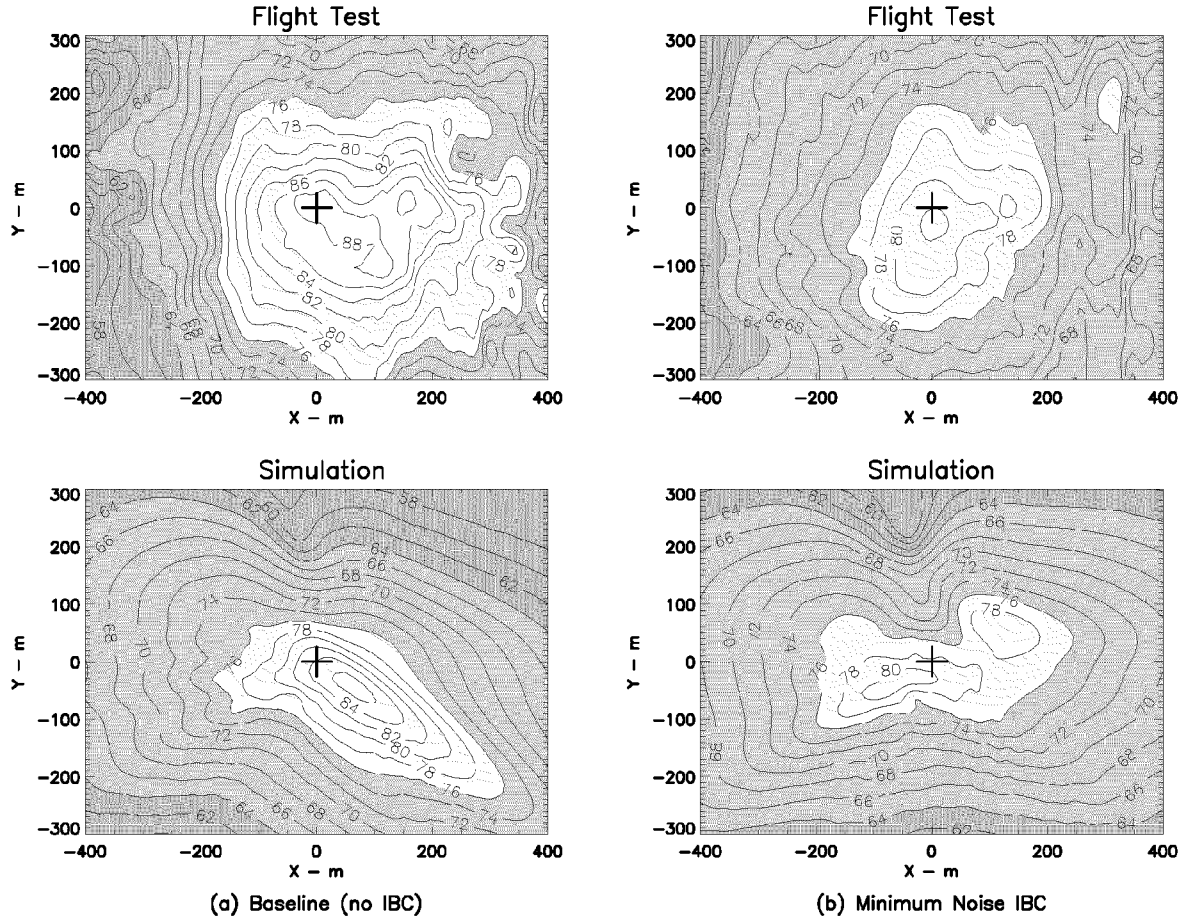

Figure 12 Measured and predicted A-weighted noise contours for (a) the baseline case (no IBC) and for (b) minimum noise 2/rev IBC settings of Fig. 11. Flight conditions as for Fig. 5

Compared to Fig. 10 (a), the tip vortices appear to penetrate the rotor disk at larger azimuth angles on the advancing side (at about ψ = 90° in the measurement and at 75° in the simulation) and at smaller azimuth angles (at ψ = 270° in the measurement) on the retreating side. The entire area downstream is mostly free from BVI traces because the vortices are below the rotor disk there and that is the reason why the noise emission is largely reduced. A similar behaviour was found for 3/rev HHC control in the wind tunnel [6]. Thus, the important parallel BVI occurring at about ψ = 50° in the baseline condition has no significant effect any more, since this vortex now is displaced below the rotor there. The essential behaviour of the tip vortex flight path, namely to penetrate the rotor disk at larger azimuth on the advancing side (where the blade-vortex interaction angle is large and BVI noise radiation low) is computed well.

3/rev and Mixed-Mode IBC Comparisons: Flight test and simulation results in terms of LA_{MAX} levels are illustrated and compared in Figures 14 (a) and 14 (b), respectively, for the variation of both a 3/rev IBC phase angle (at θ_3 = 0.6°) and a 5/rev phase angle (at θ_5 = 0.7°) for mixed mode 3/rev + 5/rev IBC inputs (at fixed 3/rev control settings θ_3 = 0.4° and ϕ_3 = 270°). Although the phase increments of 90° are rather large, BVI noise minima are measured at ϕ_3 = 278° (nominal value 270°) for the 3/rev input and at ϕ_5 = 79° (nominal value 90°) for the mixed-mode input for both flight test and simulation results. In the 3/rev IBC simulation, an optimum noise reduction benefit of nearly 5 dBA is predicted for ϕ_3 = 270°, which is in very good agreement with the HART wind tunnel results [6], but, compared to the flight test, the optimum noise reduction appears overestimated by approximately 3 dBA.

It is interesting to note here that, in the HART wind tunnel experiment, a 3/rev control amplitude of 0.85° and 3/rev phase variation increments of $\Delta\phi$ = 30° were used. In this way and in the controlled environment of the DNW, a second noise minimum was found for a phase angle corre-

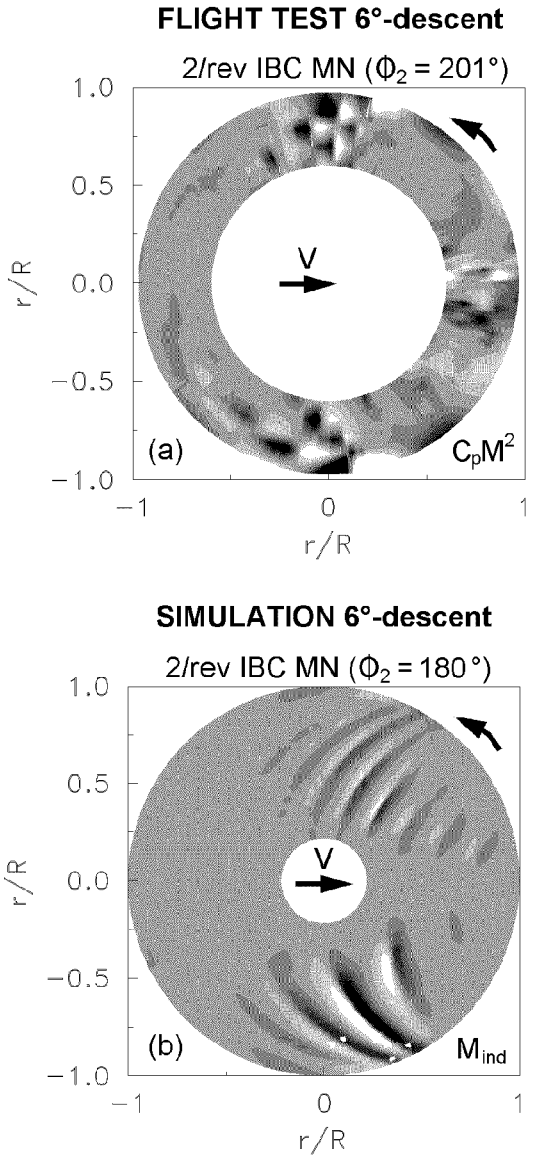

Figure 13 Comparison of (a) the leading edge blade pressure distribution C_pM^2 of the flight test to (b) the computed induced velocity distribution M_{ind} for the 2/rev IBC minimum noise case. Data h.p. filtered at 6/rev; rotor condition as for Fig. 5

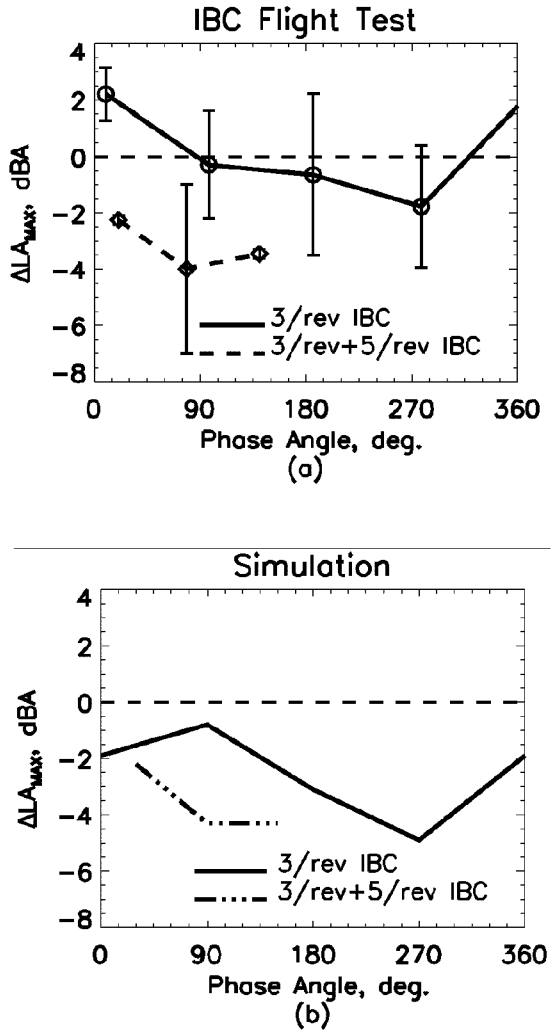

Figure 14 Comparison of (a) measured and (b) predicted A-weighted noise levels for a variation of 3/rev IBC phase angle and of 5/rev phase angle for mixed mode 3/rev + 5/rev IBC input. Flight conditions as for Fig. 5

sponding to ϕ_3 = 120° (of the phase angle definition used here), which could neither be found in the flight test nor in the simulation; it probably might have been missed because of the coarse phase increments employed here or it might have been reduced or eliminated due to the different rotor trim conditions between wind tunnel and flight test as discussed earlier.

The 3/rev + 5/rev mixed-mode case, however, shows excellent agreement of measured and predicted noise reduction benefit of about 4 dBA, a magnitude comparable to the 2/rev IBC results. The noise directivity from flight test and simulation also compares well, as is shown in Figure 15 for the mixed-mode minimum noise case (ϕ_5 = 79°) of Fig. 14.

Again, it appears that the lateral directivity on the retreating side is somewhat underestimated in the simulation due to the absence of the tail rotor noise contribution.

The partly very good and partly less satisfactory agreement between theory and experiment is mainly caused by the restricted testing time available and the resulting limited number of valid

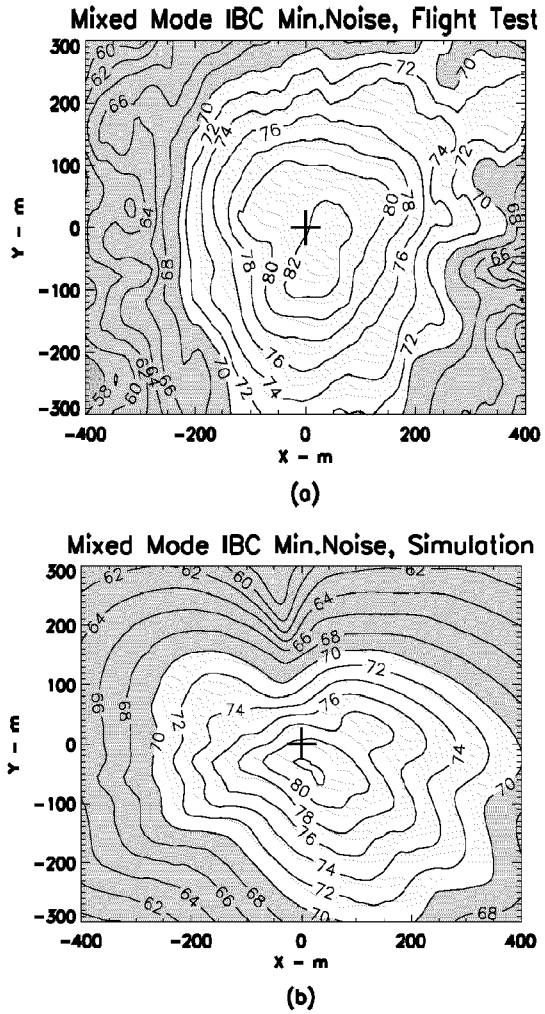

Figure 15 Comparison of (a) measured and (b) predicted A-weighted noise contours for the mixed mode minimum noise case of Fig. 14 (θ_3 = 0.4°, ϕ_3 = 270°; θ_5 = 0.7°, ϕ_5 = 79°). Flight condition as for Fig. 5 or Fig. 14, respectively

test flights per flight condition giving rise to partly large confidence intervals for the averaged experimental values; consequently, the quantitative test results have to be considered with some care. However, the general trends of the BVI noise emission and reduction potential with IBC variations indicate good agreement between flight test and simulation.

Conclusions

A joint open-loop IBC flight test programme was successfully conducted to study among other objectives the potential of individual blade root pitch control to reduce BVI impulsive noise and vibrations of a real helicopter. An upgraded IBC system with ± 1.2° control authority was installed together with extensive measurement equipment on the BO 105 S1 test aircraft, which was flown over an extended microphone array on the ground. The acoustic measurements were synchronised to the flight track and the on-board acquired data.

Precise flight path tracking to accurately define aircraft position, velocity, and flight path angle were found to be indispensable for acoustic data correction and interpretation. Selected test results quantifying the noise reduction potential of the IBC technique have been presented and compared to numerical simulation results allowing for the following conclusions:

(1) The effects of open-loop IBC variations employing harmonic 2/rev through 5/rev and multi-harmonic inputs on BVI impulsive noise, blade pressures, cabin vibrations, and on rotor trim and performance data have successfully been measured.

(2) A significant BVI noise reduction potential has been demonstrated confirming earlier full-scale and model-scale wind tunnel results.

(3) BVI noise predictions based on rotor aeroacoustic simulations correlate well with the measured noise levels and directivity patterns for most IBC variations.

(4) 2/rev IBC experimental and simulation results reveal the most promising potential for

- BVI noise reduction over a large range of IBC phase angles,
- optimum noise reduction benefit of more than 5 dBA,
- simultaneous noise and vibration reduction.

(5) 3/rev IBC experimental data base appears to be too small for substantiated conclusions concerning the noise reduction potential; simulation results compare better with model rotor wind tunnel results.

(6) 3/rev + 5/rev mixed-mode IBC results yield comparable noise and vibration reduction benefit like 2/rev IBC and are found in good agreement with simulation results.

(7) All test data, in particular the acoustic and blade pressure data, are highly useful for the development and validation of a robust controller for closed-loop IBC applications.

Acknowledgements

The RACT/IBC flight test programme was supported by the German "Bundesministerium für Bildung und Forschung" (BMBF). The authors want further to express their gratitude to the many unnamed specialists from the different partner organisations who combined their expertise to make this complex flight test campaign a success. Our special thanks go to Mr. Döring of Dornier Fairchild, who provided the PLASI indispensable for the approach flight tests.

References

[1] Brooks, T. F.: "Studies of Blade-Vortex Interaction Noise Reduction by Rotor Blade Modification", in: Proc. NOISE-CON 93, Noise Control in Aeroacoustics, Williamburg, VA, 1993

[2] Yu, Y. H.; Gmelin, B.; Splettstoesser, W. R.; Philippe, J. J.; Prieur, J.; Brooks, T. F.: "Reduction of Helicopter Blade-Vortex Interaction Noise by Active Rotor Control Technology", Progress in Aerospace Science, Vol. 33, pp. 647-687, 1997

[3] Brooks, T. F.; Booth, E. R.; Jolly, J. R.; Yeager, W. T. and Wilbur, M. L.: "Reduction of Blade-Vortex Interaction Noise Through Higher Harmonic Pitch Control", Journal of the American Helicopter Society, Vol. 35, No. 1, 1990

[4] Splettstoesser, W. R.; Schultz, K. J.; Kube, R.; Brooks, T. F.; Booth, E. R.; Niesl, G.; Streby, O.: "A Higher Harmonic Control Test in the DNW to Reduce Impulsive BVI Noise", Journal of the American Helicopter Society, Vol. 39, No. 4, 1994

[5] Polychroniadis, M.; Achache, M.: "Higher Harmonic Control: Flight Tests of an Experimental System on SA349 Research Gazelle", 42nd Annual Forum of the American Helicopter Society, Washington, DC, 1986

[6] Splettstoesser, W. R.; Kube, R.; Wagner, W.; Seelhorst, U.; Boutier, A.; Micheli, F.; Mercker, E. and Pengel, K.: "Key Results from a Higher Harmonic Control Aeroacoustic Rotor Test (HART) in the German-Dutch Wind Tunnel", Journal of the American Helicopter Society, Vol. 42, Nr. 1, 1997

[7] Kube, R.; Achache, M.; Niesl, G. and Splettstoesser, W. R.: "A Closed-Loop Controller for BVI Impulsive Noise Reduction by Higher Harmonic Control, in: 48th Annual Forum of the American Helicopter Society, Washington, D.C., 1992

[8] Niesl, G.; Swanson, S. M.; Jacklin, S. A.; Blaas, A.; Kube, R.: "Effect of Individual Blade Control on Noise Radiation", AGARD Aeroacoustics Conference, Berlin, Germany, 1994

[9] Richter, P.; Eisbrecher, H. D. and Kloeppel, V.: "Design and First Tests of Individual Blade Control Actuators", in: 16th European Rotorcraft Forum, Glasgow, U.K., 1990

[10] Swanson, S. M.; Jacklin, S. A.; Blaas, A.; Kube, R.; Niesl, G.: "Individual Blade Control Effects on Blade-Vortex Interaction Noise", 50th Annual Forum of the American Helicopter Society, 1994

[11] Jacklin, S. A.; Blaas, A.; Teves, D. and Kube, R.: "Reduction of Helicopter BVI Noise, Vibration and Power Consumption through Individual Blade Control", 51st Annual Forum of the American Helicopter Society, 1995

[12] Schimke, D.; Jänker, P.; Blaas, A.; Kube, R.; Schewe, G.; Kessler, C.: "Individual Blade Control by Servo-Flap and Blade Root Control – a Collaborative Research and Development Programme", 23rd European Rotorcraft Forum, Dresden, Germany, 1997

[13] Schimke, D.; Arnold, U.; Kube, R.: "Individual Blade Root Control Demonstration – Evaluation of Recent Flight Tests", 54th Annual Forum of the American Helicopter Society, Washington, D.C., 1998

[14] Dieterich, O.: "Application of Modern Control Technology for Advanced IBC System", 24th European Rotorcraft Forum, Marseille, France, 1998

[15] Honert, H.; van der Wall, B.; Fritzsche, M.; Niesl, G.: "Real Time BVI Noise Identification from Blade Pressure Data", Paper AC 08, 24th European Rotorcraft Forum, Marseilles, France, 1998

[16] Schöll, E.; Gembler, W.; Bebesel, M.; Splettstoesser, W.; Kube, R.; Pongratz, R.: "Noise Reduction by Blade Root Actuation – Analysis of Flight Test and Wind Tunnel Tests", Paper TE 06, 24th European Rotorcraft Forum, Marseilles, France, 1998

[17] Splettstoesser, W. R.; Niesl, G.; Cenedese, F.; Nitti, F.; Papanikas, D. G.: "Experimental Results of the European HELINOISE Aeroacoustic Rotor Test", Journal of the American Helicopter Society, Vol. 40, No. 2, 1995

[18] Van der Wall, B. G.: "Analytical Model of Unsteady Profile Aerodynamics and its Application to a Rotor Simulation Program", 15th European Rotorcraft Forum, Amsterdam, The Netherlands, 1989

[19] Beaumier, P.; Prieur, J.; Rahier, G.; Spiegel, P.; Demargne, A. (ONERA); Tung, C.; Gallmann, J. M.; Yu, Y. H. (AFDD), Kube, R.; van der Wall, B. G.; Schultz, K. J.; Splettstoesser, W. R. (DLR); Brooks, T. F.; Burley, C. L. (NASA); Boyd, D. D. (Lockheed): "Effect of Higher Harmonic Control on Helicopter Rotor Blade-Vortex Interaction Noise: Prediction and Initial Validation", AGARD-CP-552, 1995

[20] Petot, D.; Arnaud, G.; Harrison, R.; Stevens, J.; Teves, D.; van der Wall, B. G.; Young, C.; Szichinyi, E.: "Stall Effects and Blade Torsion – an Evaluation of Predictive Tools", 23rd European Rotorcraft Forum, Dresden, Germany, 1997

[21] Heller, H.; Buchholz, H.; Schultz, K. J.; Ahmed, S. R.; Splettstoesser, W.: "Helicopter Rotor Blade Aeroacoustics: A Comparison of Model-Scale Wind Tunnel and Full-Scale Flight Test Results", in: Proc. ICAS '96, Sorrent, Italy, 1996

Paper #30

Q by Chris Fielding: One of your figures showed a very good match between simulated and flight test results, but showed a fairly constant 20degree phase shift. Do you have an explanation for this phase offset ?

A (W. R. Splettstoesser): The simulation is based on a prescribed wake including effects of dynamically varying lift distribution as it is created by HHC or IBC. Due to locally increased or reduced lift, the appropriate downwash at that area is increased or reduced, leading to additional wake deflections which in reverse are important for BVI miss distance - the driving parameter for increase or reduction of BVI noise. Since the modelling is of low order, the principle effects are captured, but the accuracy with respect to control phase is as observed in the range of 20 degrees; in terms of rotor azimuth it is just 10 degrees. More cannot be expected in the current state of the model.